Bioorganic & Medicinal Chemistry Letters 21 (2011) 3813–3817

Contents lists available at ScienceDirect

Bioorganic & Medicinal Chemistry Letters

journal homepage: www.elsevier.com/locate/bmcl

Synthesis and SAR studies of novel 2-(6-aminomethylaryl-2-aryl-4-oxo-quinazolin-3(4*H*)-yl)acetamide Vasopressin V_{1b} receptor antagonists

Susan E. Napier [a,*], Jeffrey J. Letourneau [b,*], Nasrin Ansari [b], Douglas S. Auld [b], James Baker [c], Stuart Best [c], Leigh Campbell-Wan [c], Ray Chan [b], Mark Craighead [d], Hema Desai [b], Koc-Kan Ho [b], Cliona MacSweeney [c], Rachel Milne [d], J. Richard Morphy [a], Irina Neagu [b], Michael H. J. Ohlmeyer [b], Jack Pick [a], Jeremy Presland [a], Chris Riviello [b], Heather A. Zanetakos [b], Jiuqiao Zhao [b], Maria L. Webb [b]

[a] *Department of Chemistry, MSD, Newhouse, Lanarkshire ML1 5SH, UK*
[b] *Ligand Pharmaceuticals, Inc., 3000 Eastpark Boulevard, Cranbury, NJ 08512, USA*
[c] *Department of Pharmacology, MSD, Newhouse, Lanarkshire ML1 5SH, UK*
[d] *Department of Molecular Pharmacology, MSD, Newhouse, Lanarkshire ML1 5SH, UK*

ARTICLE INFO

Article history:
Received 24 February 2011
Revised 3 April 2011
Accepted 6 April 2011
Available online 13 April 2011

Keywords:
V1b
HPA
Antagonist

ABSTRACT

Synthesis and structure–activity relationships (SAR) of a novel series of vasopressin V_{1b} antagonists are described. 2-(6-Aminomethylaryl-2-aryl-4-oxo-quinazolin-3(4*H*)-yl)acetamide have been identified with low nanomolar affinity for the V_{1b} receptor and good selectivity with respect to related receptors V_{1a}, V_2 and OT. Optimised compound **16** shows a good pharmacokinetic profile and activity in a mechanistic model of HPA dysfunction.

Hyperactivity of the hypothalamic–pituitary–adrenal (HPA) axis is a neuroendocrine abnormality that has been reported to occur in a number of psychiatric conditions.[1] Arginine vasopressin (AVP) and corticotrophin releasing hormone (CRH) are the primary driving forces behind activation of the HPA axis and act in synergy to induce adrenocorticotropic hormone (ACTH) release from anterior pituitary corticotrophs. The role of AVP in regulation of the HPA axis is mediated by vasopressin V_{1b} receptor located in the pituitary. There are strong data to indicate that hyperactivity of the HPA axis during chronic stress and in depression is caused by a shift towards a predominant AVP/V_{1b} regulation of this system.[2] Antagonists of the pituitary (peripheral) V_{1b} receptor are proposed to normalise HPA overactivity and, as such, could provide therapeutic benefit in the treatment of diseases characterised by an excessive cortisol secretion such as major depression and stress-related disorders.[3] Further support for this hypothesis has come from discovery of the V_{1b} antagonist SSR149415 which has been demonstrated to inhibit AVP-induced ACTH release in vivo and showed activity in animal models predictive of antidepressant and anxiolytic activity after systemic administration.[4] Recently a series of selective V_{1b} antagonists was reported by GSK.[5]

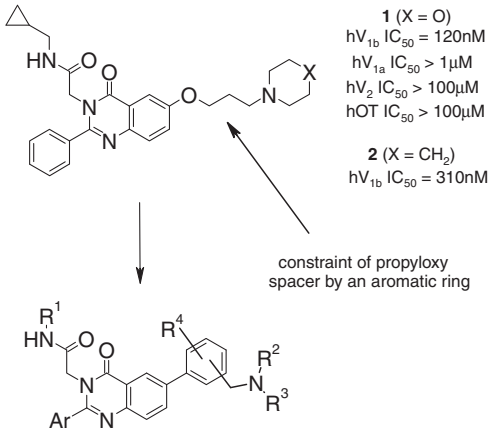

Figure 1. Constraint *via* aryl linker.

We recently reported details of our hit-to-lead optimisation effort around a novel series of 2-(4-oxo-2-aryl-quinazolin-3(4*H*)-yl)acetamides as vasopressin V_{1b} receptor antagonists.[6] This effort gave rise to lead compounds **1** and **2** (Fig. 1). Although **1** and **2**

* Corresponding authors.
E-mail addresses: susan.napier@spcorp.com, susannapier67@googlemail.com (S.E. Napier), Jeffrey_letourneau@yahoo.com (J.J. Letourneau).

0960-894X/$ - see front matter © 2011 Elsevier Ltd. All rights reserved.
doi:10.1016/j.bmcl.2011.04.022

showed improved physicochemical properties compared to other known competitor ligands, the propyloxy spacer between the quinazolinone and amine functionality was somewhat flexible (i.e., five rotatable bonds). As part of our SAR exploration driven by our desire to identify compounds with improved V_{1b} affinity, conformational constraints were explored in this region of the molecule. A number of approaches to reduce the number of rotatable bonds were investigated and here we report replacement of the propoyloxy spacer with an aryl substituent (Fig. 1).

The compounds appearing in Tables 1–5 were synthesised via the general route outlined in Scheme 1.[7] 2-Amino-5-bromobenzoic acid **3** was reacted with glycine amide **4** under standard amide coupling conditions to afford intermediate **5**. Conversion of **5** to intermediate quinazolinones **7** was performed by condensation with an appropriately substituted aryl imidate salt **6**, readily prepared from the corresponding aryl nitrile. Bromo intermediate **7** was reacted with bis(pinacolato)diboron in the presence of $PdCl_2$(dppf) to afford boronate **8**. Suzuki coupling with substituted bromobenzaldehydes **9** then provided aldehydes **10** which were subsequently converted to products **11** by reductive amination with an appropriate amine.

The compounds in Tables 1–5 were evaluated for their ability to displace the binding of tritium labelled arginine vasopressin ([^{3}H]-AVP) to human V_{1b} receptor in a whole cell binding assay using CHO/human V_{1b}/VIP-Luciferase cells and 5 nM [^{3}H]-AVP.[8] SAR generated during our hit-to-lead activities demonstrated the importance for binding affinity of a basic amine functionality on the propyloxy sidechain.[6] Due to the rigid nature of the aryl spacer compared to the propyloxy spacer, a preliminary investigation was performed to establish the preferred position of the aminomethyl moiety for optimal binding affinity (Table 1). Substitution in the *meta* position was found to be optimal with substitution in the *ortho* and *para* positions resulting in inactive compounds. Interestingly, **11c** and **11d** demonstrated improved binding affinity versus their respective congeners **1** and **2** containing the propyloxy spacer. Compound **11d**, substituted with piperidin-1-ylmethyl in the *meta* position, showed a five-fold increase in V_{1b} affinity (IC_{50} = 60 nM) compared to compound **2** (IC_{50} = 310 nM) and **11c**, *meta* substituted with morpholin-1-ylmethyl, showed a more modest 1.5-fold increase (IC_{50} = 79 nM) over **1** (IC_{50} = 120 nM).

The active *meta*-isomers were our focus for further investigation. Although **11d** had moderate V_{1b} affinity, the physicochemical properties required optimisation and the first objective was to lower MW and *c*log*P* (**11d**: MW = 506.7, *c*log*P* = 5.8). A set of amines were surveyed aimed at lowering MW compared to **11d** (Table 2).

Table 1
Positional isomers of the aminomethyl moiety

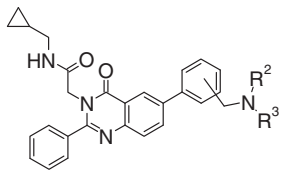

11a-11f

Compds	Position	NR^2R^3	hV_{1b} IC_{50}[a] (nM)
11a	*ortho*	Morpholin-1-yl	>20,000
11b	*ortho*	Piperidin-1-yl	>20,000
11c	*meta*	Morpholin-1-yl	79 (±35)
11d	*meta*	Piperidin-1-yl	60 (±4)
11e	*para*	Morpholin-1-yl	>20,000
11f	*para*	Piperidin-1-yl	>20,000

[a] Values are means of two experiments, standard deviation is given in parentheses.

Table 2
Survey of lower MW amine groups

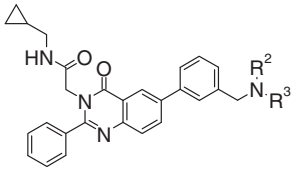

12a-12g

Compds	NR^2R^3	hV_{1b} IC_{50} (nM)[a]	MW	*c*log*P*[9]
11d		60 (±4)	506.7	5.8
12a		1200 (±300)	438.5	3.8
12b		320 (±80)	452.6	4.2
12c		314 (±28)	466.6	4.6
12d		540 (±112)	494	5.7
12e		275 (±177)	478.6	4.7
12f		388 (±181)	492.6	5.3
12g	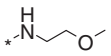	642 (±298)	496.6	4.2

[a] Values are means of two experiments, standard deviation is given in parentheses.

Table 3
Optimisation of amide moiety

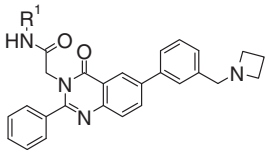

13a-13f

Compds	R^1	hV_{1b} IC_{50} (nM)[a]	MW	*c*log*P*[9]
12e		275 (±177)	478.6	4.7
13a		2350 (±1768)	466.6	4.8
13b		1044 (±504)	480.6	5.2
13c		397 (±40)	466.6	4.6
13d		187 (±160)	480.6	5.0
13e		2550 (±496)	464.6	4.1
13f		238 (±20)	492.6	5.2

[a] Values are means of two experiments, standard deviation is given in parentheses.

Substitution with smaller amine functionality generally resulted in a reduction in affinity compared to **11d** and appeared to correlate with the lower lipophilicity of these compounds. Compounds **12c** and **12e** both showed a ~five-fold decrease in affinity but the

Table 4
2-Phenyl substitution

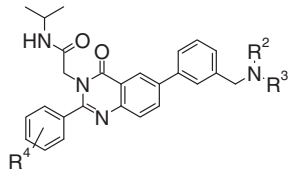

14a-14h

Compds	R^4	NR^2R^3	hV_{1b} IC_{50} (nM)[a]	MW	*clogP*[9]
14a	3-OMe		9(±4)	484.6	4.5
14b	3-OMe		46 (±21)	496.6	4.6
14c	3-OMe		2 (±0)	524.7	5.7
14d	3-Cl		19 (±8)	489.0	5.2
14e	3-Cl		60 (±35)	501.0	5.3
14f	3-Cl		9 (±1)	529.1	6.4
14g	2-OMe		610 (±7)	496.6	4.6

[a] Values are means of two experiments, standard deviation is given in parentheses.

Table 5
Modification to aryl spacer

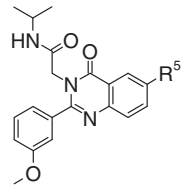

15a-15f

Compds	R^5	hV_{1b} IC_{50} (nM)[a]	MW	*clogP*[9]
14a	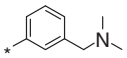	9 (±4)	484.6	4.5
15a	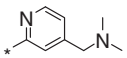	52 (±12)	485.6	3.2
15b	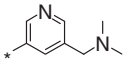	77 (±36)	485.6	3.0
15c	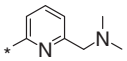	37 (±13)	485.6	3.2
15d	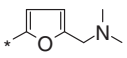	700 (±110)	474.6	3.9
15e	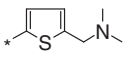	500 (±100)	490.6	4.4
15f	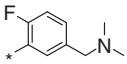	7 (±2)	502.6	4.7

[a] Values are means of two experiments, standard deviation is given in parentheses.

reduction in affinity was offset by the improvement in *clogP* and MW compared to **11d** (**12c**: MW = 466.6, *clogP* = 4.6; **12e**: MW = 478.6, *clogP* = 4.7). Compound **12e** was chosen as a starting point for further optimisation.

Next our focus turned to optimisation of the alkyl amide portion of the molecule. Unlike SAR described during optimisation of the propyloxy spacer series, the nature of the amide substituent appeared not to have such a dramatic effect on affinity.[10] Substitution with *n*-propyl **13a**, isobutyl **13b**, or cyclopropyl **13e** resulted in a nine-, four- and 11-fold decrease in affinity compared to **12e**, respectively (Table 4). Substitution with a bulky, α-branched isopropyl **13c**, *tert*-butyl **13d** or cyclopentyl **13f** group gave comparable V_{1b} affinity to **12e**. In the case of the isopropyl analogue **13c** we had managed to further reduce MW with minimal reduction in affinity.

Next we concentrated on substitution of the phenyl ring at the C(2)-position of the quinazolinone (R^4). It had been demonstrated in the propyloxy spacer series that substitution in the 3-position of the phenyl ring could substantially enhance V_{1b} affinity, particularly if with a 3-methoxy- or 3-chloro- substituent.[9] A similar boost in affinity through 3-substitution was observed in the aryl spacer series (Table 4). When NR^2R^3 was azetidin-1-yl (**14b** and **14e**), an eight-fold increase in affinity was observed when R^4 = 3-methoxy **14b** (IC_{50} = 46 nM compared to **13c** IC_{50} = 397 nM) and a six-fold increase when R^4 = 3-chloro **14e** (IC_{50} = 60 nM). When NR^2R^3 was dimethylamino, a more dramatic increase in affinity was observed with **14a** (R^4 = 3-methoxy) having an IC_{50} at V_{1b} of 9 nM and **14d** (R^4 = 3-chloro) having an IC_{50} of 19 nM. Good affinity was also observed when NR^2R^3 was piperidin-1-yl with **14c** (R^4 = 3-methoxy) and **14f** (R^4 = 3-chloro) having IC_{50}s of 2 and 9 nM, respectively. The high *clogP* and high MW of **14c** and **14f** was, however, considered prohibitive for further development. *ortho*-Substituted analogue **14g** (R^4 = 2-methoxy) was also prepared and the poor affinity of this compound confirmed the SAR trend observed in the propyloxy spacer series where 3-substitution was preferred.[9] Compound **14a** was identified for further investigation possessing good V_{1b} affinity (44-fold increase over **13c**) and moderate *clogP* and MW.

Finally we investigated modification of the aryl spacer (Table 5). Replacement with pyridyl (**15a**, **15b** and **15c**) provided a favourable reduction in *clogP* but unfortunately resulted in a three- to eight-fold drop in affinity compared to **14a**. Replacement with five-membered heterocycles such as furanyl **15d** and thiophenyl **15e** was disfavoured, both having >50-fold lower affinity than **14a**. Analogues with substitution on the aryl spacer were also studied, with the *ortho*-fluoro (*ortho*-with respect to the quinazolinone scaffold) analogue **15f** retaining V_{1b} affinity comparable to **14a** (IC_{50} = 7 nM).

Compounds **14a** and **15f** were tested in vitro for their metabolic stability in human liver microsomes (HLM) and also for their caco-2 permeability (Table 6). Both compounds showed good permeability in a Caco-2 permeability assay, but disappointingly displayed only moderate intrinsic clearance (CL_{int}) in HLM. It was hypothesised that metabolism was occurring in the 2-aryl region of the molecule with metabolite ID studies indicating metabolism was occurring by oxidation rather than *O*-demethylation of the methoxy substituent. To this end additional substitution around the 2-aryl ring with fluoro- as a blocking group was investigated in **14a**, which was chosen over **15f** based on its lower initial lipophilicity (Fig. 2). Compound **16** containing a 4-fluoro substituent was identified exhibiting excellent stability in HLM, CL_{int} <12 μL/min/mg (RLM, CL_{int} = 26 μL/min/mg) and acceptable caco-2 permeability. Additionally **16** had improved V_{1b} affinity over **14a**. Compound **16** was shown to be a V_{1b} antagonist in a luciferase

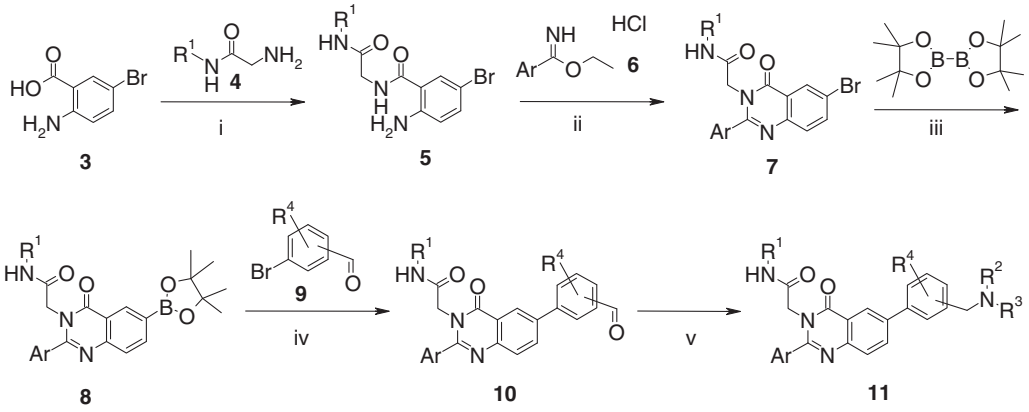

Scheme 1. Reagents and conditions: (i) EDCI, HOBt, DIPEA, DMP, room temperature; (ii) EtOH, 75 °C; (iii) KOAc, $PdCl_2$(dppf), DMF, 80 °C; (iv) $Pd(PPh_3)_4$, K_3PO_4, DMF, 80 °C; (v) HNR^2R^3, DCE, $NaBH(OAc)_3$, AcOH (cat.), room temperature.

Table 6
Evaluation of compounds **14a** and **15f** for HLM stability and Caco-2 permeability

Compd	HLM CL_{int} (μL/min/mg)	Caco-2 Papp (AB/BA) (nm/s)
14a	45	141/227
15f	58	121/233

Table 7
Pharmacokinetic parameters for **16** in male Wistar rats

Route, dose[a]	iv (1 mg/kg)	po (5 mg/kg)
Clearance (mL/min/kg)	40.2 ± 11.1	
Elimination half life (h)	1.61 ± 0.10	
V_{ss} (L/kg)	4.85 ± 1.23	
AUC (ng/ml h)	441 ± 112[b]	930 ± 880[c]
F%		45 ± 43

[a] Vehicle for iv dosing is 10% (v/v) DMA in water and for po dosing is 5% (v/v) mulgofen in saline.
[b] AUC_{inf}.
[c] AUC_t.

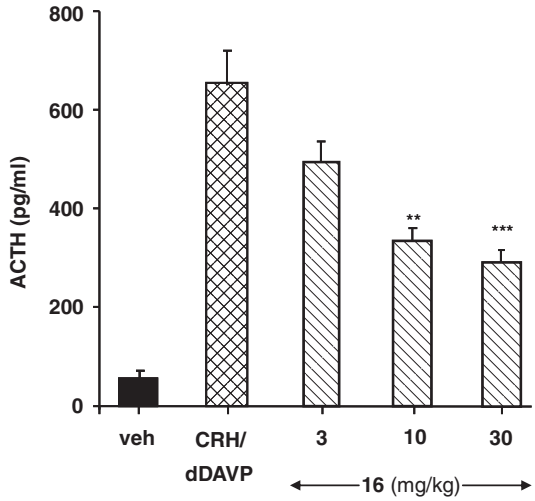

Figure 3. In vivo profiling of **16** in a rat model of HPA hyperactivity. p <0.05; $^{**}p$ <0.005; $^{***}p$ <0.001 versus CRF/dDAVP.

reporter assay linked to AVP-mediated intracellular calcium mobilisation (data not shown) and demonstrated excellent selectivity (>10,000-fold) over human V_{1a}, V_2 and OT receptors and against a broad panel of biological targets at Novascreen (GPCRs, ion channels, transporters and enzymes; <50% displacement of binding or inhibition at 2.5 μM).

The pharmacokinetics of **16** after oral and intravenous dosing were determined in male Wistar rats (Table 7). Compound **16** showed moderate clearance and high V_{ss} in keeping with its physicochemical properties, leading to a moderate elimination half life of 1.6 h. Compound **16** exhibited a moderate oral bioavailability of 45%. Additionally the CYP inhibition profile for **16** was promising (IC_{50} values at main human drug metabolising CYPs >17 μM).

Compound **16** was profiled in a model of HPA hyperactivity.[11] Upon administration to rats, desmopressin (dDAVP, a mixed V_{1b}/V_2 agonist) and CRH (a CRH_1/CRH_2 agonist) work synergistically to elicit the release of ACTH. Pretreatment with a V_{1b} antagonist can attenuate this release of ACTH. Compound **16** was dosed orally 2 h prior to treatment with dDAVP and CRH. As illustrated in Figure 3, there was a dose-dependent reduction in ACTH release, indi-

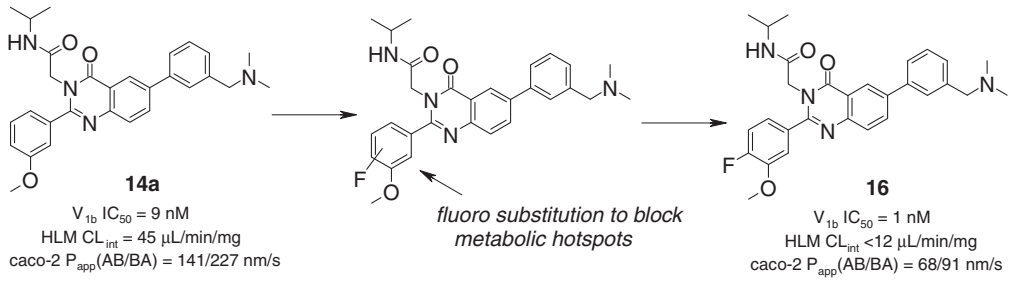

Figure 2. Effect of aryl fluoro substitution on HLM stability

cating that **16** can antagonise the effects of dDAVP in vivo at 10 mg/kg p.o.

In conclusion, a series of V_{1b} antagonists exemplified by lead compounds **1** and **2** were further optimised through replacement of the propoyloxy spacer with a more conformationally constrained aryl spacer. Successful optimisation with respect to V_{1b} affinity and in vitro ADME profile was achieved. Compound **16** was identified having nanomolar affinity for V_{1b} and excellent selectivity with respect to V_{1a}, V_2 and OT receptor subtypes and against a broad panel of unrelated targets (Novascreen). Compound **16** showed a promising pharmacokinetic profile in rat and was further profiled in an in vivo model of HPA hyperactivity where it was demonstrated to antagonise the effects of dDAVP on elevating ACTH levels in rat.

References and notes

1. (a) Holsboer, F.; Barden, N. *Endocr. Rev*. **1996**, *17*, 187; (b) Barden, N.; Reul, J. M. H. M.; Holsboer, F. *TINS* **1995**, *18*, 6; (c) Dinan, T. G.; O'Brien, S.; Lavelle, E.; Scott, L. V. *Psychol. Med.* **2004**, *34*, 169.
2. (a) Scaccianoce, S.; Muscolo, L. A. A.; Cigliana, G.; Navarra, D.; Nicolai, R.; Angelucci, L. *Endocrinology* **1991**, *128*, 3138; (b) Ma, X.-M.; Levy, A.; Lightman, S. L. *Endocrinology* **1997**, *138*, 4351.
3. (a) Scott, L. V.; Dinan, T. G. *Life Sci.* **1998**, *62*, 1985; (b) Aquilera, G.; Rabdan-Diehl, C. *Regul. Pept.* **2000**, *96*, 23.
4. (a) Griebel, G.; Simiand, J.; Serradeil-Le Gal, C.; Wagnon, J.; Pascal, M.; Scatton, B.; Maffrand, J.-P.; Soubrie, P. *PNAS* **2002**, *99*, 6370; (b) Serradeil-Le Gal, C.; Wagnon, J.; Tonnerre, B.; Roux, R.; Garcia, G.; Griebel, G.; Aulombard, A. *CNS Drug Rev.* **2005**, *11*, 53.
5. Arban, R.; Bianchi, F.; Buson, A.; Cremonesi, S.; Fabio, R.; Gentile, G.; Micheli, F.; Pasquarello, A.; Pozzan, A.; Tarsi, L.; Terreni, S.; Tonelli, F. *Bioorg. Med. Chem. Lett.* **2010**, *20*, 5044.
6. Letourneau, J. J.; Riviello, C.; Li, H.; Cole, A. G.; Ho, K.-K.; Zanetakos, H. A.; Desai, H.; Zhao, J.; Auld, D. S.; Napier, S. E.; Thomson, F. J.; Goan, K. A.; Morphy, J. R.; Ohlmeyer, M. H. J.; Webb, M. L. *Bioorg. Med. Chem. Lett.* **2010**, *20*, 5394.
7. Letourneau, J.; Riviello, C.; Ho, K.-K.; Chan, J.-H.; Ohlmeyer, M.; Jokiel, P.; Neagu, I.; Morphy, J. R.; Napier, S. E. PCT Int. Appl. WO 06095014, 2006.
8. *V_{1b} whole cell binding assay*. The assay was performed in a 96-well format. CHO cells stably expressing human V_{1b} receptor were cultured at 37 °C with 5% CO_2 in DMEM/F12 (Invitrogen) with 10% FBS (HyClone Labs, FetalClone II, #206007), 0.4 mg/mL G418 (Invitrogen) and 1% penicillin and streptomycin (Invitrogen). Cells were seeded at 30,000 cells into either 384-well (50 μL/well) or 96-well (100 μL/well) clear bottom plate and cultured at 37 °C overnight. Cells were washed twice with 100 μL/well (for 384-well plate) or 200 μL/well (for 96-well plate) of PBS. For initial HTS, 384-well plates containing dried down compounds were resuspended with 30 μL/well of 5 nM [^{3}H]-AVP in assay buffer (PBS with 10 mM $MgCl_2$, 0.1% BSA and 1% DMSO. After solubilisation, 20 μL/well was transferred from compound plate to cell plate. For compound affinity, test compounds were initially serially diluted in DMSO and then intermediately diluted at 1:50 with assay buffer (PBS with 10 mM $MgCl_2$ and 0.1% BSA). To each well, 25 μL of serially diluted compounds were added followed by 25 μL of 10 nM [^{3}H]-AVP in assay buffer. The final reaction contained 5 nM [^{3}H]-AVP and 1% DMSO. The mixtures were incubated at room temperature for 30 min. The plates were washed twice with 100 μL/well (for 384-well plate) or 200 μL/well (for 96-well plate) of PBS and air dried. The amount of radioactivity remaining was determined by adding 50 μL of scintillation fluid and shaking for 30 min followed by counting for 1 min/well in a Perkin–Elmer Microbeta.
9. clog*P* 4.3, BioByte Corp. 201W. 4th St., #204 Claremont, CA 91711-4707, USA.
10. Napier, S. E.; Letourneau, J. J.; Ansari, N.; Auld, D. S.; Baker, J.; Best, S.; Campbell-Wan, L.; Chan, H.; Cole, A. G.; Craighead, M.; Desai, H.; Goan, K. A.; Ho, K.-K.; Hulskotte, G. J.; MacSweeney, C. P.; Milne, R.; Morphy, J. R.; Neagu, I.; Ohlmeyer, M. H. J.; Peeters, A. W. M. M.; Presland, J.; Riviello, C.; Ruigt, G. S. F.; Thomson, F. J.; Zanetakos, H. A.; Zhao, J.; Webb, M. L. *Bioorg. Med. Chem. Lett.* **2011**, *21*, 1871.
11. Rats were orally administered either vehicle (5% mulgofen in saline) or compound at the appropriate dose at $T = 0$. At $T + 100$ min CRH (0.3 μg/kg) or 0.9% phoshpate buffered saline (PBS) was administered through a jugular vein catheter. Desmopressin (dDAVP; 0.5 mg/kg) or PBS was administered iv via the catheter at $T + 120$ min. At $T + 130$ min a 0.5 ml blood sample was collected. Samples were stored on ice immediately after collection and then centrifuged (2500 rpm, 4 °C, 15 min). Plasma was extracted and stored at −40 °C. Samples were then analysed for drug and ACTH concentrations by mass spectroscopy and enzyme-linked immunosorbent assay (ELISA: IDS U.K.), respectively.